EXPERIMENTAL RESULTS: CHARGE-STATE- AND CURRENT-DENSITY DISTRIBUTIONS AT THE PLASMA ELECTRODE OF AN ECR ION SOURCE

L. Panitzsch*, T. Peleikis, M. Stalder, R.F. Wimmer-Schweingruber

Institute for Experimental and Applied Physics (IEAP), University of Kiel, Germany

Abstract

We have measured the current-density distribution (CDD) in very close vicinity (15 mm downstream) of the plasma electrode of our hexapole-geometry electron-cyclotron-resonance ion source (ECRIS). For this, we equipped our 3D-movable puller electrode with a customized Faraday Cup (FC) inside. To achieve high spatial resolution we reduced the aperture of the puller electrode to only 0.5 mm. Thus, the source-region of the extracted ion beam is limited to a very small area of the plasma electrode's hole (d = 4 mm). The information about the charge-state distribution (CSD) and the current density in the plane of the plasma electrode is conserved in the ion beam and was scanned by remotely moving the small-aperture puller electrode (incl. FC) across the aperture of the plasma electrode. From additional m/q-measurements for the different positions we can deduce that different ion charge-states are grouped into bloated triangles of different sizes but with the same orientation in the plane of the plasma electrode with the current density peaking at the centre. This confirms simulations by various groups as well as some emittance measurements, but adds spatial resolution for the different charge-states.

INTRODUCTION

To further understand the processes within the plasma of ECR ion sources various groups have developed simulation tools to predict different plasma parameters or to benchmark them against existing ion sources. The parameters of importance usually are the extractable current, the achievable charge states, and the emittance of the beam at the extraction. The simulations also show the spatial arrangement of the different ion species and charge states. Here, the highly charged ions are concentrated closer to the axis of symmetry than the lower-charged ion species, but always arranged in characteristically shaped triangular stars [1, 2, 3] (if operated with a hexapole for radial plasma confinement). As a result the highly charged ions are expected to have a lower emittance. This was substantiated by emittance measurements using a bending magnet for ion separation [4, 5]. Unfortunately, using this technique the spatial information is lost. Therefore, we use a different approach to determine the spatially resolved CSD in the plane of the plasma electrode by experiment: We use our 3D-movable puller electrode to record the profile (or CDD) of the extracted beam at a distance of only 15 mm to the plasma electrode. Knowing the total CSD of the extracted

beam and the axial magnetic fields we can conclusively show (by now for charge states 2+ to 4+) that the different charge states are grouped into triangular structures with the same orientation but different sizes in the plane of the plasma electrode. The current density peaks at the center.

BEAM PROFILE MEASUREMENTS CLOSE TO THE EXTRACTION

To measure beam profiles at a distance of only 15 mm (!) downstream of the plasma electrode we take advantage of our 3D-movable puller electrode to scan the plasma electrode's aperture. It is equipped with a customized FC. The aperture which spatially limits the measured ions has a diameter of only 0.5 mm. The dimensions of the plasma electrode and the plasma chamber are shown in fig. 1. The geometrical dimensions of the FC and the use of a negatively biased repeller guarantee the suppression of secondary electron escape. Beam profiles have been aquired for two different source settings. By adding helium into the plasma chamber we changed the ion composition and the pressure inside the ECR zone. Therefore, we separate between the settings RG (residual gas at 5E-7 mbar) and RGHe (helium added until 1E-6 mbar) in the following paragraphs. The resulting beam profiles are shown in fig. 2. The figure shows the CDD for both settings (RG left and RGHe right) in the plane of the puller electrode at comparatively high resolution. The x- and y-axes denote the position in the plane of the plasma electrode with the origin being at beam center. The colour bars indicate the measured current densities. For both measurements we see similar tendencies: Areas with similar current densities can be grouped into bloated triangular-like structures with different orientations and sizes overlapping each other. The
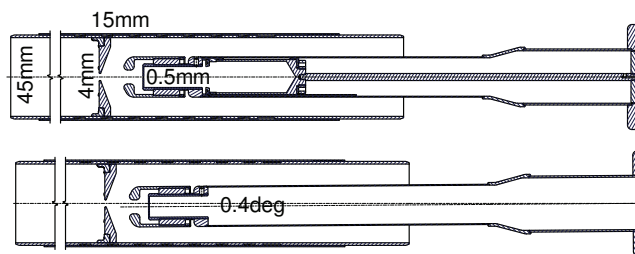

Figure 1: CAD-drawings of the plasma chamber, the plasma electrode, and the puller electrode for different settings: (1) central with implemented FC, (2) at the outmost position without the FC. Here the puller electrode is tilted by 0.4 °. The resulting shift is 2 mm.
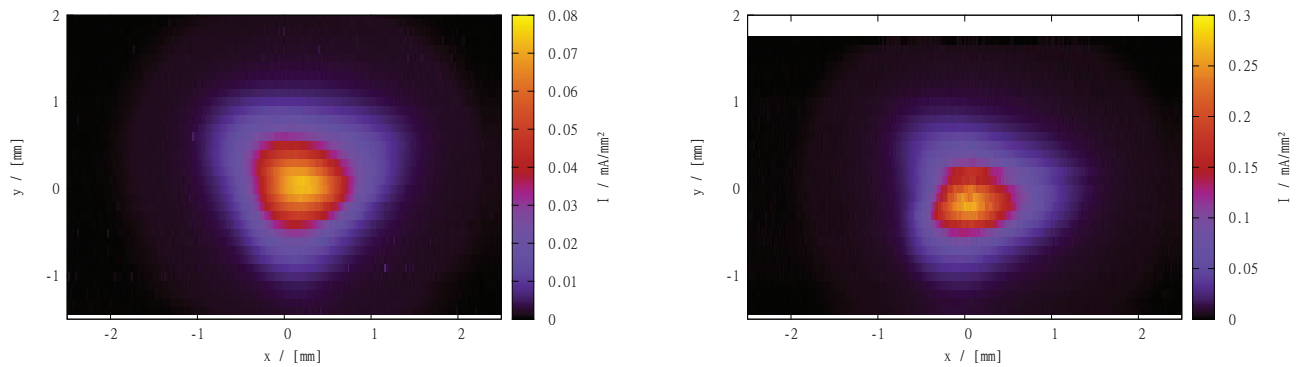
* panitzsch@physik.uni-kiel.de

Figure 2: Measured current density distributions (CDDs or profiles) shortly behind the plasma electrode for settings RG (left) and RGHe (right). Note that the colour bars are scaled differently to match the particular intensity range.[2]

total current density is peaking at the center. In addition, the circular shape of the plasma electrode is clearly visible and its diameter can be verified to be 4 mm. Slight deviations from an ideal circle are supposed be caused by the end-position switch triggering the start signal of the current recordings. As we clearly can resolve the circular shape of the plasma electrode as well as the triangular structures we conclude that the ions passing through the tiny aperture are indeed extracted from a very limited region of the neutral plasma sheath only. If the ions were extracted from larger regions the resulting figures would be blurred and we would not be able to clearly resolve them. For the identification of the single structures we need further information about the CSD of the total extracted ion beam and the magnetic fields. With that, we will show that each of these triangular structures is dominated by ions of one m/q-ratio and that their orientation is equal directly at the extraction as predicted by the simulations referred above.

SPATIALLY RESOLVED CHARGE-STATE DISTRIBUTION (CSD)

To determine the spatially resolved CSD as observable from behind the sector magnet we again used the puller electrode with reduced diameter (but without the FC). We analyzed the m/q-spectra of the beams extracted from the different regions of the plasma electrodes aperture (and therefore the neutral plasma sheath) by the use of a sector magnet. The thus obtained spatially resolved CSDs for the most dominant ion species (N and O) are presented in fig. 3 for setting RG. We have to point out that these distributions are strongly influenced by the transmissivities of the particular charge states which was optimized before. All measurements were performed at an extraction voltage of 7 kV at an axially fixed position of the puller electrode (the puller electrode was only moved in the plane perpendicular to the beam axis, again). The results shown here have to be regarded as a 'snapshot' looked at from behind the sector magnet for the applied focussing only.

Figure. 3 shows the spatial distributions for the different nitrogen (left-hand) and oxygen (right-hand) charge states in the range from 1+ to 4+. Higher charged ion species were only found at the exactly central position. The intensities in the individual plots are scaled to the maximum measured intensity, I_{max}. I_{max} is indicated at the top of the individual plots and increases from low to high charge states. In both settings (RG and RGHe with only RG being shown here) the highest charge states only fill the central pixel and therefore seem confined to the very central region of the plasma electrode. As the emittances of the higher-charged ion species were measured to be smaller than for the low-charged ions (as referred to above, [4, 5]) we would expect the higher-charged ions to have a higher transmissivity also when being extracted from the non-central regions. Though, these ions are only present in the spectra recorded with the puller electrode at exactly central position. This, indeed, is a hint for them to be concentrated close to the axis of the source as observed in many simulations (again, as referred to before). With decreasing charge state the distribution broadens and nearly fills the plasma aperture for doubly charged ions. Obviously, the highest charge states clearly peak in the centre while lower charge states populate areas with larger radii around the centre. Also, the recorded current densities peak at the centre and decline with increasing radial distance for each ion species. The slope of the decline is distinctly steeper for more highly charged ions and more shallow for the lower charged species. From these spatially resolved CSDs we have calculated the total CSD of all extracted ions by summing up the currents for each particular ion species. The resulting CSDs for both settings (RG and RGHe) are presented in fig. 4. We observe a shift in the charge state with highest intensity from 2+ (for setting RG) to 3+ or 4+ for setting RGHe. This seems to be the effect of gas mixing. To validate these results we compared these calculated CSDs extracted with the puller electrode with reduced diameter with CSD measurements performed with our standard-sized puller electrode (not shown within these proceedings). The CSDs recorded with both different extraction techniques nicely show the same character-
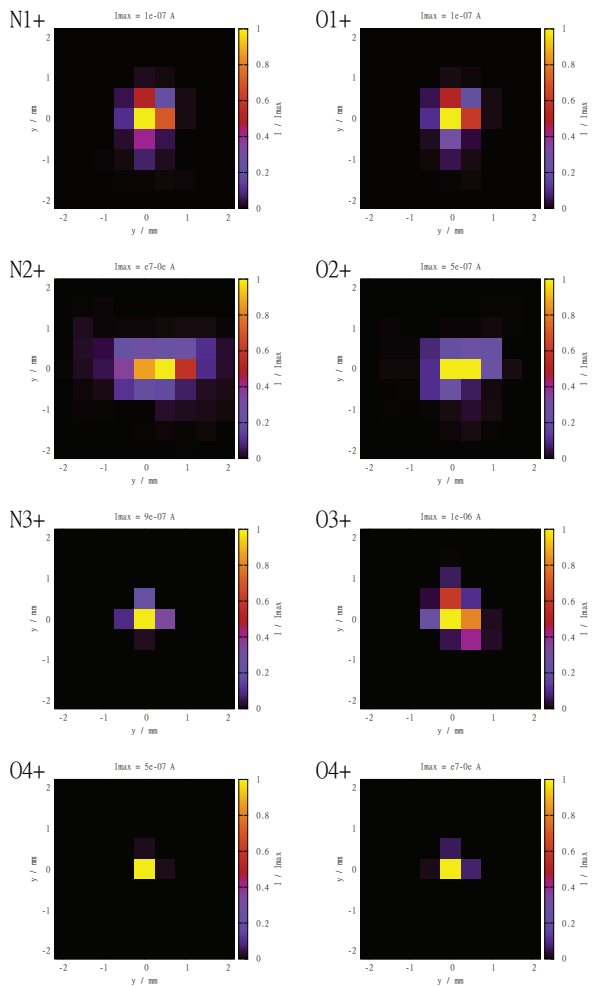
Figure 3: Measured charge state distributions at the plasma electrode as visible from behind the sector magnet for setting RG (residual gas only). The x- and y-axes denote the position in the plane of the plasma electrode with the origin being at beam centre. The colours show the measured current densities scaled to the maximum detected current, I_{max}, for each graph. This allows visualization of the entire distribution.[2]

istics/trends. Therefore, we can conclude that the transmissivity of the small-aperture puller electrode is not worse compared to the standard extraction and systematical ion-optical errors can be excluded. We even observed a 'multi-aperture-like' effect. Multi-aperture extractions are known to result in significantly increased total currents [7]. The added currents extracted with the puller electrode with reduced aperture at many different positions in the plane of the plasma electrode are higher than the currents detected with the standard-sized puller electrode (not shown in these proceedings, see [6] for reference). This trend was observed for all charge states higher than 1+.
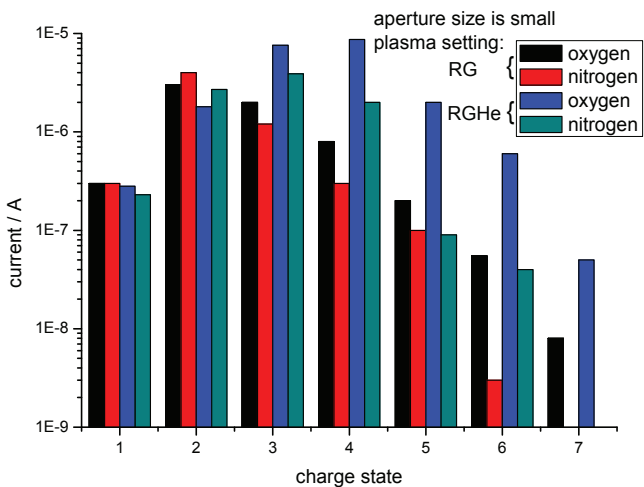

Figure 4: Comparison of the total charge state distributions for settings RG and RGHe. The distribution for the small sized aperture is calculated from the results of the CSD measurements by summing up the currents for each particular ion species. With helium as a mixing gas we see a shift of the maximum ($2+ \rightarrow 3+$ or $4+$) in the total charge state distribution and an increase of all higher charge states.[2]

COMBINATION OF THE PREVIOUS RESULTS

In this section we combine the results of the CSD measurements with the results of the CDD measurements. Taking the magnetic fields into account we are able to deduce the distribution of the different ion species directly at the extraction. We begin with a short discussion of systematic errors and the validity of the results: The CDDs are recorded using a FC inside the puller electrode. This results in a very short drift distance for the ion beam. For geometrical reasons the aperture size of the puller electrode in combination with the inner diameter of the FC guarantee the capture of the total beam passing through the aperture. The use of a repeller in front of the FC restricts secondary electrons from escape. A magnetic field-induced rotation has to be considered but generally we can exclude systematic errors for the CDD measurements. For the spatially resolved CSD measurements we have to point out limited validity. The presented CSDs portray only a 'snapshot' for the current focussing settings. They can be regarded as source regions in the plane of the plasma electrode for the different ion species effectively transmitted through the sector magnet under the particular focussing. A change in the extraction voltage will change the presented distributions due to ion-optical reasons. Therefore the calculated total CSDs (fig. 4) represent only the ion species that are transmitted through the sector magnet. They do not necessarily represent the real totally extracted CSD which we are interested in for our subsequent analyses. We know that the transmissivities for the standard and the tiny-sized apertures of the puller electrode are nearly identical (as
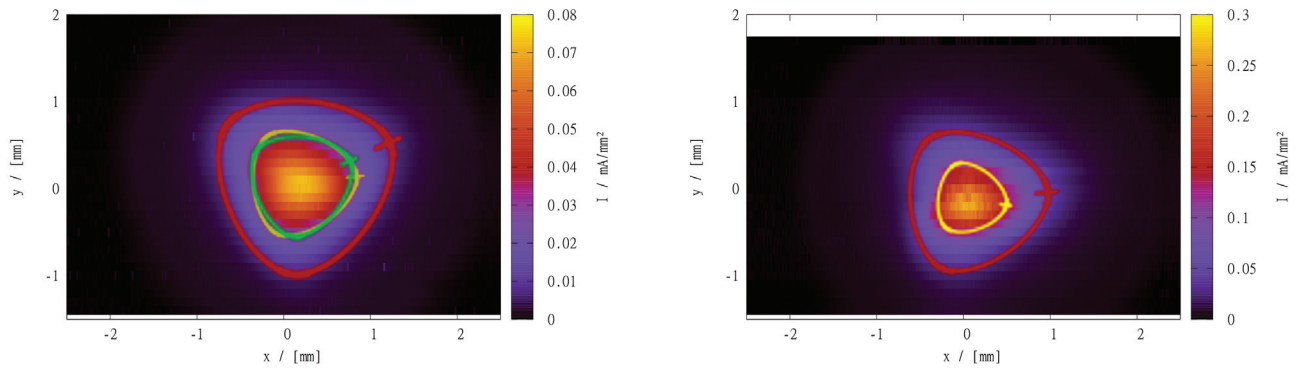
Figure 5: Measured CDD for settings RG and RGHe (compare caption of fig. 2 for details). Here the detected structures are framed with marked bloated triangles to guide the eyes. Note the different color scales.

mentioned above). Thus, we have determined multiple total CSDs for beams extracted with the large puller electrode while varying the extraction voltage. The spectra show that the main trends (especially the dominating ion species) within the recorded total CSDs do not differ significantly within the checked voltage range (4 kV to 11 kV) from these shown in fig. 4 (for 7 kV). Accordingly, we use the total CSDs already presented in fig. 4 for the following argumentation.

In fig. 2 the CDD in close vicinity of the extraction is shown. Here, bloated triangular structures of different sizes and orientations are clearly visible but no information about the ionic composition is present. To solve this we consult the (caluclated total) CSDs (fig. 4) obtained from the spatially resolved CSD measurements (fig. 3). The structures visible in fig. 2 should mainly be populated by the dominating ion species of the particular setting. For the analysis we make the assumption that higher charge states are concentrated closer to the axis. For setting RG the most dominant ion species are charged 2+ and 3+ with the 2+ component being slightly more dominant. Setting RGHe is dominated by charge states 3+ and 4+, respectively. Other ion species are too strongly suppressed to contribute significantly. For both settings two bloated triangles are found within the CDD. To guide the eyes we have framed the measured structures of fig. 2 by bloated triangles. These triangles have a mark to distinguish their orientation (see fig. 5). With this aid we are able to determine the angle of rotation of the different structures which is important for the analysis:

As for setting RG charge states 2+ and 3+ are dominant we assume that here the outer triangle (framed red, see fig. 5) is mainly populated by ions of charge state 2+. The orientation of the inner structure is more difficult to distinguish as different charge states (mainly 2+ and 3+) overlap each other. We are able to find two different orientations of the frames (green and yellow) that both well accentuate the inner structure(s?) of setting RG. A bloated structure in the center with the same orientation as the outer one (framed red, 2+) might still be caused by the 2+ component as for each charge state the current density is observed to

peak at the center and that particular charge state is slightly dominant. On the other hand, there surely also is a strong 3+ component present in inner, central triangle. This 3+ component might be the reason for that second, differently oriented (yellow) inner frame. For setting RGHe we see the dominance of charge states 3+ and 4+. Again, according to the observation that higher charge states seem to be populated closer to the axis we assume the outer triangle (framed red) to mainly consist of ions of charge state 3+. Therefore, the inner triangle (framed yellow) is assumed to be dominated by the 4+ component. For the red-framed structure of setting RGHe (see fig. 2, right) two facts attract attention. It is rotated and its size appears to have decreased slightly compared to the red-framed structure of setting RG. The inner (yellow-framed) structure of setting RGHe (fig. 2, right) shows both, a further rotation together with a further decrease in size.

The beam is extracted in a region where the axial magnetic field peaks at roughly 1 T. This leads to a Lorentz-force-induced rotation of the beam. The angle of rotation Θ_{tot} can be calculated with the formula [8]:

$$\Theta_{tot} = \sqrt{\frac{q}{8mU_{extr}}} \cdot \int B_z dz \qquad (1)$$

with q, m, and U being the charge, the mass, and the extraction voltage respectively. The rotation of the beam that occurs after having passed the tiny aperture of the puller electrode does not affect the CDD measurements since all ions passing the aperture at its defined position will be collected by the FC. We summarize the information gained so far in table 1. For each resolved structure we denote the assumed dominating charge state as well as the observed orientation 15 mm downstream of the plasma electrode with the vertical plane denoting 0°. In addition, we line out the calculated rotation for the different charge states. The thus deduced orientation of the structures in the plane of the plasma electrode is given as the difference of both values. We see that the orientation of all structures calculated back to the plane of the plasma electrode shows the same value ($\approx$13° ccw). This very well reproduces the orientation we observe for the sputter- and deposition marks at the inner

Figure 6: Sputter marks observed on the inner side of the plasma electrode. The tilt angle is ≈13° counter clockwise in relation to the vertical plane. This is in good agreement with the values for the original orientations calculated in table 1.

side of the plasma electrode itself (see fig. 6). This is a strong indicator that the dominating particles of the particular triangles shown in fig. 2 (or fig. 5, respectively) were assumed correctly. As a consequence we can draw the conclusion that indeed the different ion species are grouped in triangular structures of different sizes but same orientation in the plane of the plasma electrode and the current densities peak at the center. Thus, our measurements support the simulations of various groups who have predicted this behaviour.

CONCLUSIONS

We recorded beam profiles (CDDs) and spatially resolved CSDs in the closest vicinity of the plasma electrode we found in the literature (only 15 mm downstream). We combined both results in order to deduce for the CDD and the CSD directly at the extraction of a hexapole geometry ECR ion source. The results clearly show higher currents peaking at the center as well as the presence of (bloated) triangular structures. Each of these structures is dominated by ions of the same charge state. In the plane of the plasma electrode all the structures are orientated in the same direction determined by the magnetic field. The surface area of these structures differs from comparatively large for low

considered structure	suspected charge state	observed orientation	calculated rotation	original orientation
RG red	2+	-65°	-78°	+13°
RG green/yellow	2+/3+	-65°/-81°	-78°/-95°	+13°/+14°
RGHe red	3+	-81°	-95°	+14°
RGHe yellow	4+	-97°	-110°	+13°

Table 1: Summary of the information gained from the previous analyses. The observed orientation and the original orientation are given in relation to the vertical plane which denotes 0°. The original orientation is calculated as the difference of the observed orientation minus the calculated rotation.

charged ions and decreases rapidly for more highly charged ions. The higher/highest charge states clearly peak only in the centre and therefore populate the smallest effective radii. This is to our knowledge the first direct measurement of the CSD and the CDD at the extraction. The results in general conform to results from simulations and facts deduced from emittance measurements, both performed by other groups.

References

[1] C. Pierret, L. Maunoury, S. Biri, J. Y. Pacquet, O. Tuske, and O. Delferriere. Preliminary results of the ion extraction simulations applied to the mono1000 and supershypie electron cyclotron resonance ion sources. *Review of Scientific Instruments*, 79(2):02B703, 2008.

[2] L. Maunoury, C. Pierret, and J.Y. Pacquet. Extraction from ECR ion sources: a new way to increase beam brightness. In *Proceedings of ECRIS08 18th International Workshop on ECR Ion Sources*, pages 224–228, 2008.

[3] J. P. M. Beijers and V. Mironov. Three-dimensional simulations of ion dynamics in an electron cyclotron resonance ion source. *Review of Scientific Instruments*, 81(2):02A307, 2010.

[4] D Wutte, M A Leitner, and C M Lyneis. Emittance measurements for high charge state ion beams extracted from the aecr-u ion source. *Physica Scripta*, 2001(T92):247, 2001.

[5] M.A. Leitner, C.M. Wutte, and Lyneis C.M. Design of the extraction system of the superconducting ecr ion source venus. In *Particle Accelerator Conference, 2001. PAC. IEEE*, 2001.

[6] Lauri Panitzsch, Thies Peleikis, Michael Stalder, and Robert F. Wimmer-Schweingruber. Spatially resolved charge-state and current-density distributions at the extraction of an electron cyclotron resonance ion source. *Review of Scientific Instruments*, 82(9):093302, 2011.

[7] R. Geller. *Electron cyclotron resonance ion sources and ECR plasmas*. Institute of Physics Pub., 1996.

[8] W. Glaser. *Grundlagen der Elektronenoptik*. Wien, 1952.